Progress In Electromagnetics Research M, Vol. 103, 197–207, 2021

Dual-element Multiple-Input-Multiple-Output System for Sub-6 GHz (5G) and WLAN Applications with Enhanced Isolation

Anupa Chatterjee[1, *], Manas Midya[2], Laxmi P. Mishra[3], and Monojit Mitra[1]

Abstract—A dual-band two-port MIMO antenna with very high isolation is proposed for 5G/WLAN application. The overall size of the MIMO antenna is $(18 \times 44 \times 0.8)\,\text{mm}^3$. The unequal arm of the Inverted-F Antenna (IFA) is the reason for the dual bands. Bending and extending one of the arms with the staircase shape is responsible for the proposed dual-bands having resonant frequency at 3.45 GHz (3.3 GHz–3.65 GHz) and 5.1 GHz (4.8 GHz–5.5 GHz) respectively with percentage impedance bandwidth of 10% and 13.6%, respectively. The proposed antenna uses a simple decoupling structure based on a wide inverted T-shaped slot to achieve good isolation (better than 18 dB and 34 dB respectively for the dual-bands) between the ports. The envelope correlation coefficient (ECC) and channel capacity loss (CCL) are within the acceptable limits.

1. INTRODUCTION

The fifth generation wireless system, known as 5G, could be 100 times faster than 4G and will power the Internet Of Things (IOT). The 5G wireless communication system supports spectrum below 6 GHz and millimeter wave above 24 GHz. The "Sub-6" spectrum is used for many purposes because of its longer range. The Telecom Regulatory Authority of India (TRAI) and Department of Telecommunication (DOT) are expected to hold the first phase of 5G spectrum. Country's telecom operator would acquire 3.3 GHz (n78) bands in the first phase [1, 2]. The characteristics of the wireless communication systems can be improved with multiple-input-multiple-output systems. These systems have multiple input and output elements to increase the capacity of the system, even the signal fading in the multipath environment can be decreased. The key element in a MIMO system is the antenna structure. However, the close placement of the antenna elements leads to mutual coupling, thus resulting in performance degradation. The minimum distance between the antenna elements should be half of the operating wavelength for desirable isolation, but due to need of compactness, the spacing between the antenna elements is decreased. Thus, the main challenge is to achieve high isolation between closely spaced antenna elements having shared ground plane for MIMO applications.

Designing dual-band MIMO antenna is a challenging task since same isolation mechanism does not work for both the dual frequencies. In literature, several dual-band MIMO antennas have been reported. A dual-element antenna for WLAN application is studied in [3], and here the antenna elements have two radiating parts, a driven monopole, and a shorting branch. A high isolation higher than 20 dB is achieved for both the bands, and the decoupling structure consists of a protruded ground and a narrow slot etched on the ground plane. But the size of the antenna is very large. In [4], a compact dual band MIMO antenna for WLAN application is studied, where a wide slot and a pair of narrow slots

Received 10 May 2021, Accepted 16 July 2021, Scheduled 22 July 2021

* Corresponding author: Anupa Chatterjee (anupa.c12@gmail.com).

[1] Department of Electronics & Telecommunication Engineering, Indian Institute of Engineering Science & Technology, Shibpur, India. [2] Electronics & Communication Engineering Department, Institute of Engineering and Management, Gurukul Campus, Kolkata, India. [3] Department of Electronics & Communication Engineering, Siksha 'O' Anusandhan (deemed to be University), Bhubaneswar, India.

are used as a decoupling network. A multiantenna system based on two Planar Inverted-F Antennas (PIFAs) for a dual-band is proposed in [5], and two slots are inserted on the Printed Circuit Board (PCB) for proper isolation. In [6], a dual-band inverted-F MIMO antenna is studied. By involving two meandering monopoles, and WLAN bands are achieved. High isolation is achieved by etching an inverted T-slot on the ground plane and a meandering resonant branch. This meandering line technique is also proved to be effective for good isolation as studied in [7]. A compact dual-band two elements MIMO antenna for WLAN application is presented in [8], but the dimension is $30 \times 70 \times 0.8\,\text{mm}^3$. Two slots are etched in the ground plane together with two transmission lines at the top surface for isolation. A two-element dual-band MIMO antenna for WLAN is studied in [9] but again with a longer dimension of $38 \times 43 \times 1.6\,\text{mm}^3$. A 2×2 MIMO to cover 700 MHz and 2.4 GHz bands is studied in [10] with an overall dimension $58 \times 110 \times 1.56\,\text{mm}^3$. A metamaterial inspired MIMO for LTE and Wi-MAX applications is studied in [11] with an overall dimension of $43 \times 26 \times 0.8\,\text{mm}^3$. A bent T-shaped resonator embedded between two C-shaped monopole antennas increases isolation higher than 15 dB as studied in [12]. Protruded ground plane technique is proposed in [13, 14]. But all the above design occupies large space which is not suitable for smaller compact devices. A compact two-element MIMO antenna for 5G application is studied in [15], where the radiating elements are rhombus shaped with tapered microstrip line feed and a remodeled T-shaped ground stub for improved isolation. A compact wideband dual/quad element MIMO antenna for Wi-MAX and 5G application is proposed in [16] using jeans textile material, where for isolation improvement meandered line structures are integrated between the antenna elements. A PIFA pair based MIMO antenna for 5G (New Radio) bands and LTE band 46 is studied in [17]. However, the above discussed two-element MIMO antennas were mostly designed for WLAN application with large dimension and moderate isolation.

In this paper, the proposed MIMO geometry consists of two T-shaped monopole antennas, each having two unequal arms with the longer arm shorted to the ground to form the IFA structure. The other arm is bent and then further extended with the staircase structure for the desired 5G and WLAN bands. The simulation and design performance steps are presented and discussed. FR-4 is used as the dielectric substrate with relative permittivity of 4.4, thickness of 0.8 mm, and loss tangent of 0.02. In Section 2, single element analysis is done with the design evolution steps. Later, 2×2 MIMO design is analyzed with isolation improvement and diversity performance shown. The result shows good agreement between the simulation and measured results. In Section 3, equivalent circuit analysis with ADS keysight software of the proposed antenna is shown. The results of the simulated, measured and for the equivalent circuit are in good agreement. Experimental results are explained in Section 4, and lastly the paper is concluded.

2. MIMO ANTENNA DESIGN AND ANALYSIS

2.1. Single Element Antenna

Figure 1(a) illustrates the single element antenna. The unit element is used to design the proposed dual-band MIMO antenna. It has an overall size of $18 \times 20\,\text{mm}^2$ and is printed on a 0.8 mm thick FR-4 epoxy substrate, with relative permittivity of 4.4 and loss-tangent of 0.002. The design of the single element antenna is inspired from a T-shaped monopole. Unequal arms give dual band resonances. The longer arm is shorted to the ground plane to form the desired IFA structure. The other arm is bent and then extended with the staircase structure resulting in the desired dual-band frequency responses at 3.4 GHz (3.3 GHz–3.63 GHz) and 5.08 GHz (4.75 GHz–5.38 GHz). Steps of evolution are shown in Figure 2 in five steps and its performances in Figure 3.

In the first step, the longer arm of the T-shaped monopole is shorted to the ground to form the IFA-1 structure having resonances at 4.74 GHz and 6.3 GHz, respectively. In the next step, the other side is bent upward, then extended and further bent to form the IFA-2 structure, thus shifting the lower frequency to 2.95 GHz while the upper resonance is at 4.86 GHz. To include the 5G band, a 3-step staircase structure is included with IFA-2. With the 1st-step of the staircase structure (IFA-3), the resonance gets shifted to 3.1 GHz and 5.01 GHz, respectively. In IFA-4, with the 2nd step of the staircase, the resonance again gets shifted to 3.28 GHz and 5.1 GHz. Finally, with IFA-5 structure, i.e., the single element structure of the proposed MIMO antenna, the lower resonance is at 3.4 GHz (3.3 GHz–3.63 GHz)

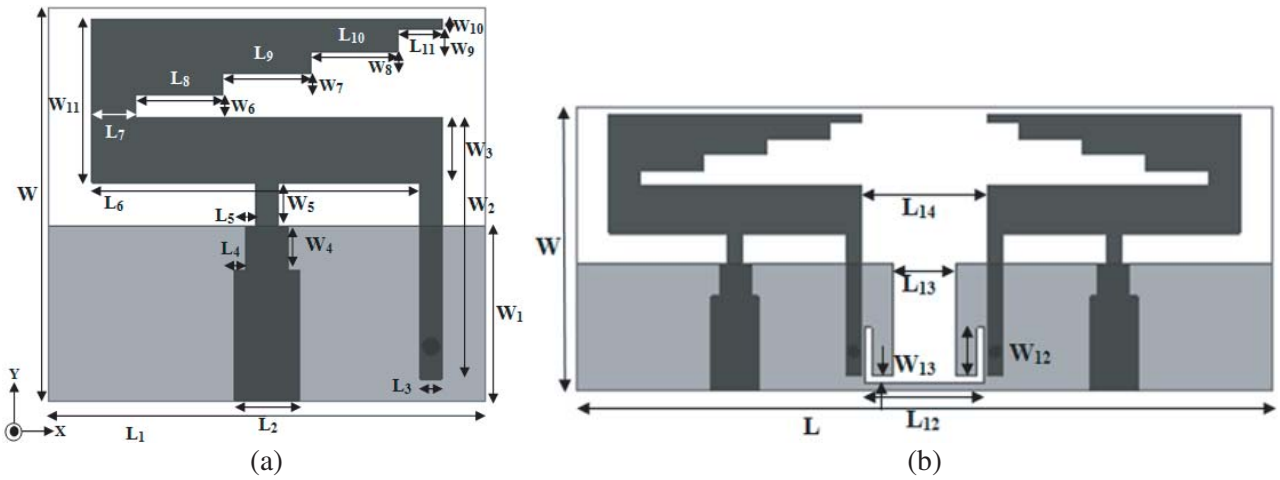

Figure 1. (a) Top view of the antenna. (b) Proposed 2×2 MIMO structure. ($W = 18$, $W_1 = 8$, $W_2 = 12$, $W_3 = 3$, $W_4 = W_5 = 2$, $W_6 = W_7 = W_8 = W_9 = 1$, $W_{10} = 0.5$, $W_{11} = 7.5$, $L_1 = 20$, $L_2 = 3$, $L_3 = 1$, $L_4 = L_5 = 0.5$, $L_6 = 15$, $L_7 = 2$, $L_8 = L_9 = L_{10} = 4$, $L_{11} = 2$, $W = 18$, $L = 44$, $L_{12} = 7.6$, $L_{13} = 4$, $L_{14} = 8$, $W_{12} = 3$, $W_{13} = 0.5$) (unit: millimeters).

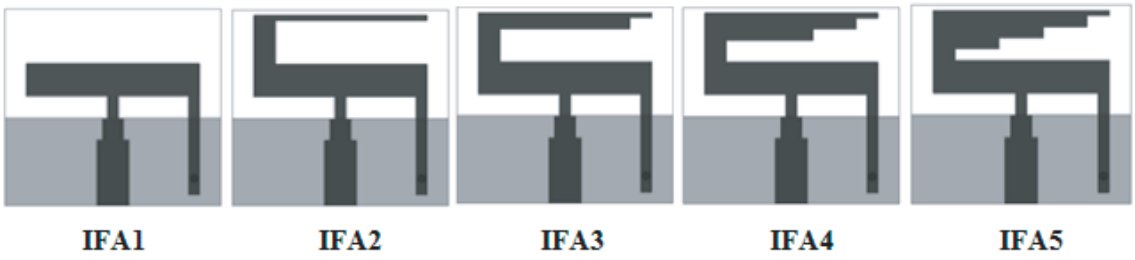

Figure 2. Evolution steps of the antenna.

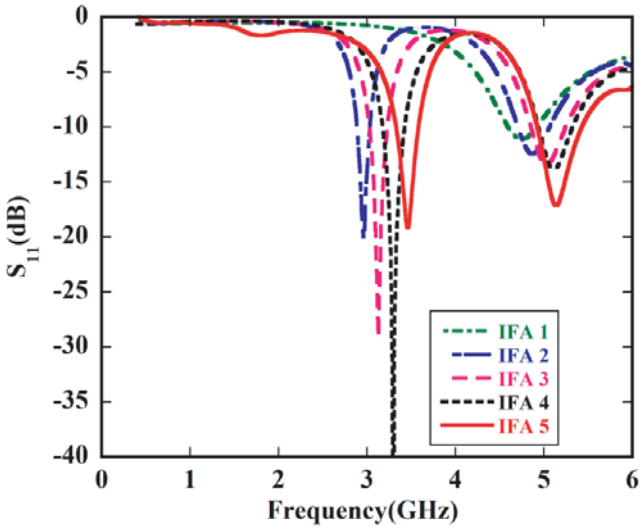

Figure 3. Reflection coefficient versus frequency for the evolution steps of the antenna.

and 5.08 GHz (4.75 GHz–5.38 GHz), respectively. Including these three steps reduces the current path, thereby shifting the lower frequency to the right side [18–20].

2.2. Proposed Two Element Quad-Band MIMO Antenna Design and Isolation Improvement

Figure 1(b) shows the proposed two-element dual-band MIMO antenna designed on a low cost FR-4 substrate. A fabricated prototype of the proposed antenna is shown in Figure 12. To evolve the configuration of the proposed antenna, four different cases are considered from Stage-1 to Stage-4 respectively as shown in Figure 4. In Stage-1, with only the partial ground plane, the result shows that the isolation is −13 dB and −16 dB, respectively. In Stage-2, a wide rectangular strip is removed from the ground plane which improves the impedance matching even the isolation is better. The mutual coupling is less than −15.7 dB and −23 dB, respectively. The slots in the ground plane perturb the surface current distribution at the ground plane such that the electromagnetic energy coupling between the two ports is reduced, and thus good isolation is achieved. In Stage-3, two smaller slots are merged with the previous wider slot to form the inverted T-structure which further improves the impedance matching. The mutual coupling is −16.9 dB and −25.7 dB, respectively. Stage-4 is the final proposed structure. With a little bit of modification of the inverted T-shaped structure, the impedance matching is improved to −18.8 dB for 3.45 GHz and −17 dB for 5.1 GHz, respectively. Even the isolation is improved between the two antenna elements to −18 dB and −34 dB, respectively. Since the radiating elements are identical, the transmission and reflection coefficients are identical. The S-parameters of the proposed MIMO antenna and the corresponding $|S_{21}|$-parameters for all the four stages are shown in Figure 5 and Figure 6, respectively. Thus, the results are satisfactory for MIMO applications in 5G/WLAN bands.

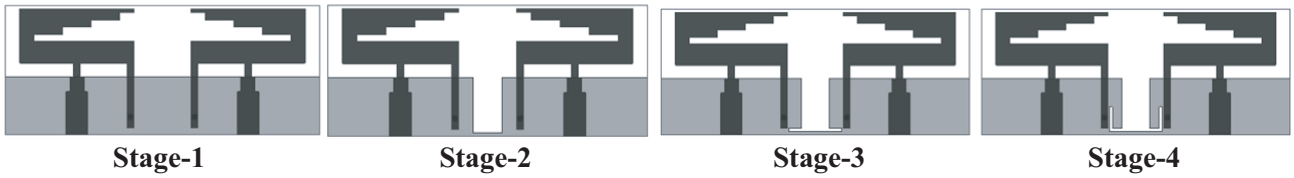

Figure 4. Evolution of the proposed MIMO antenna.

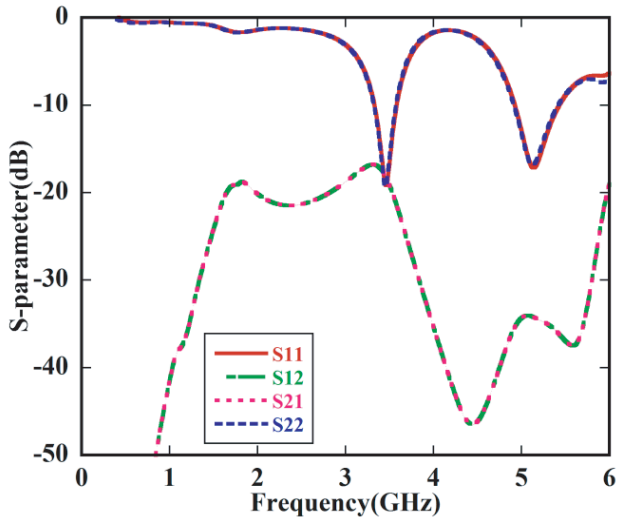

Figure 5. Simulated $|S|$-parameters of the proposed MIMO antenna

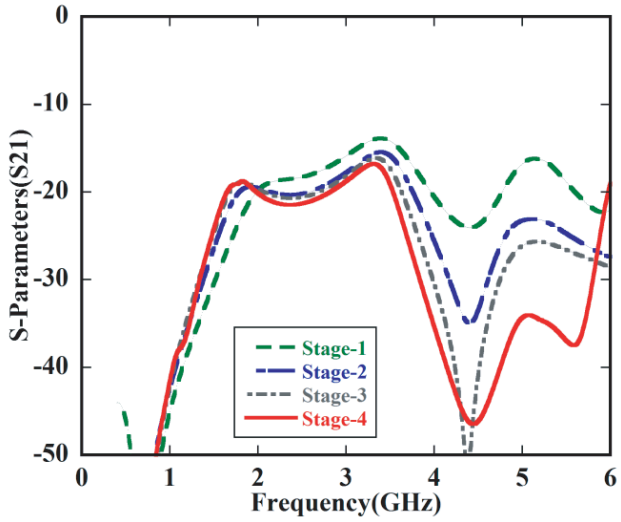

Figure 6. Simulated $|S_{21}|$ parameters of Stage-1, Stage-2, Stage-3 and Stage-4.

2.3. Surface Current Distribution

To understand the simultaneous improvement in the impedance matching and isolation, surface current distribution is plotted on the surface of ground plane and radiating surface for the dual frequencies for all the four stages of improvement of MIMO antenna when port-1 is excited while port-2 is matched in terminated load as shown in Figures 7–8. A significant amount of surface current flows on the surface of ground plane between the two antenna elements. To reduce mutual coupling, the separation between the antenna elements can be increased. But for space constraint, instead of increasing the separation, a wide vertical slot is etched on the ground plane. The isolation is increased with introduction of the vertical slot since the surface currents are suppressed. A horizontal slot of $L_{12} \times W_{13}$ is etched on the ground plane below the vertical slot. This further resists the surface current to flow from the ground plane of ANT-1 to the ground plane of ANT-2. Thus more isolation between ports is observed. From comparing the surface current distributions at 3.45 GHz and 5.1 GHz for all the four stages, it can be seen that the coupling from ANT-1 to ANT-2 is reduced greatly in Stage-4. The minimum isolation achieved for 3.45 GHz is −18 dB and for 5.1 GHz is −34 dB, respectively.

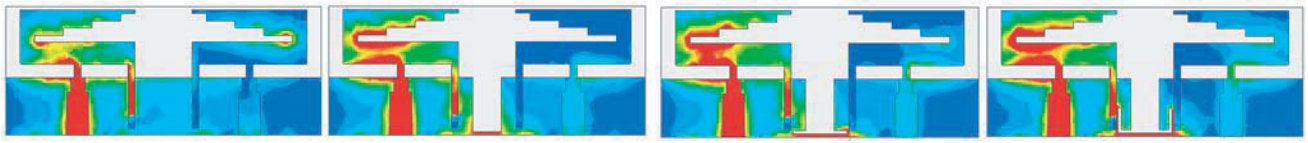

(a) (b) (c) (d)

Figure 7. Surface current on (a) Stage-1, (b) Stage-2, (c) Stage-3, (d) Stage-4 at 3.45 GHz when port-1 is excited.

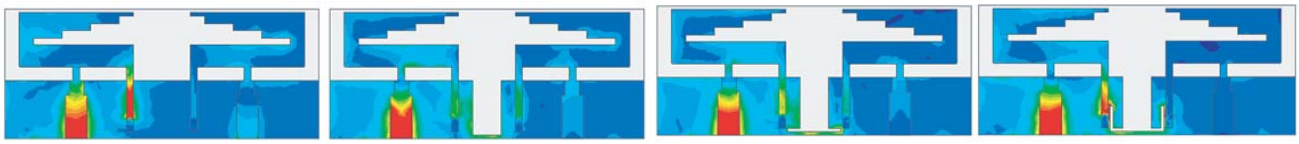

(a) (b) (c) (d)

Figure 8. Surface current on (a) Stage-1, (b) Stage-2, (c) Stage-3, (d) Stage-4 at 5.1 GHz when port-1 is excited.

2.4. Diversity Performance

Envelope correlation coefficient (ECC) is an important parameter to analyze the performance of a MIMO antenna. But ECC involves all the scattering parameters to show their effects on the correlation coefficient. Lower is the value of ECC less is the correlation between the two antenna elements. If ECC is zero, then the two antenna elements are isolated from each other while ECC equals one means that there is coupling between the antenna elements. Thus the range of ECC lies between zero and one. An expression of ECC in terms of S-Parameters for any practical lossy MIMO antenna is given by [3].

$$ECC = \frac{|S_{ii}^* S_{ij} + S_{ji}^* S_{jj}|^2}{\left(1 - |S_{ii}|^2 - |S_{ji}|^2\right)\left(1 - |S_{jj}|^2 - |S_{ji}|^2\right)_{\rho_{rad,i}\rho_{rad,j}}} \tag{1}$$

$$DG = 10\sqrt{1 - |ECC|^2} \tag{2}$$

where $\rho_{rad,I}$ and $\rho_{rad,j}$ are the radiation efficiencies of the i-th and j-th antennas, respectively. The acceptable unit of ECC is less than 0.5. For the proposed antenna, the value of ECC is 0.002 as shown in Figure 9. Diversity Gain (DG) is defined as the difference between the power level in dB of the combined signal within the diversity antenna system and that of a single antenna system in one

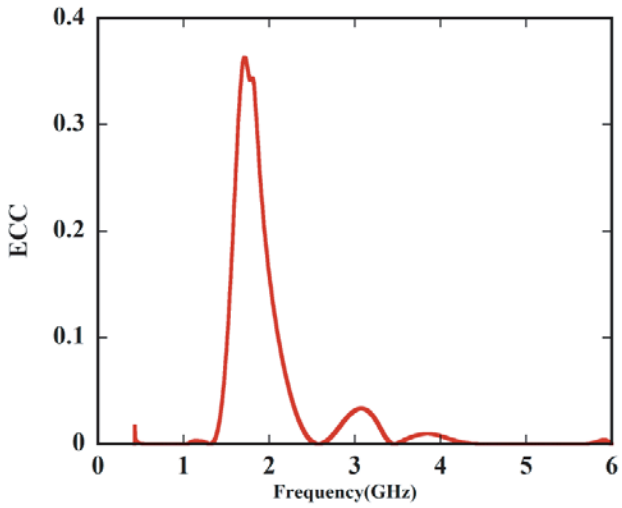

Figure 9. Simulated Envelope correlation coefficient (ECC) of the proposed MIMO antenna.

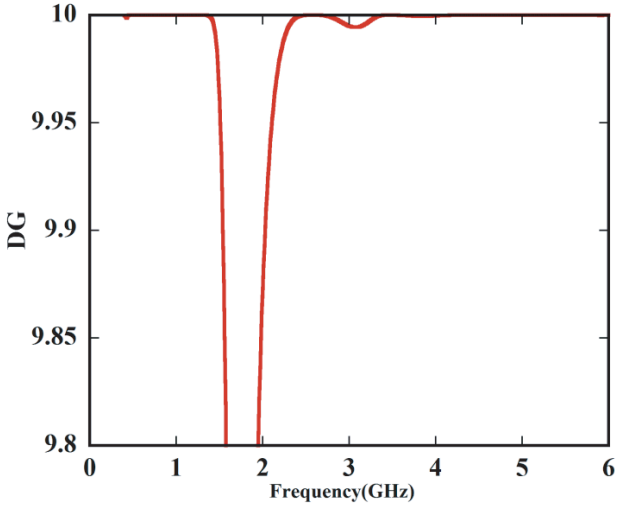

Figure 10. Simulated Diversity gain (DG) of the proposed MIMO antenna.

diversity channel [21, 22]. The relation between ECC and DG is represented using Equation (2). The proposed MIMO structure gives DG value around 9.9 dB. Figure 10 shows the simulated DG.

Another important parameter is Channel Capacity Loss (CCL) used to characterize the quality of the MIMO antenna. It ensures the transmission of the information with maximum rate over the channel without any distortion. The CCL parameter (C_{LOSS}) is determined by Equation (3) as given in [22].

$$C_{LOSS} = -\log_2 \det\left(\beta^R\right) \tag{3}$$

$$\text{where } \beta^R = \begin{bmatrix} \beta_{ii} & \beta_{ij} \\ \beta_{ji} & \beta_{jj} \end{bmatrix} \tag{4}$$

$$\beta_{ii} = 1 - \left(\sum_{j=1}^{N} |S_{ij}|^2 \right. \tag{5}$$

$$\beta_{ji} = -\left(S_{ii}^* S_{ij} + S_{ji}^* S_{jj}\right) \tag{6}$$

Simulated CCL is plotted in Figure 11. It is observed that the obtained CCL is less than 0.5 bps/Hz for the dual operating frequencies.

3. EQUIVALENT CIRCUIT MODELING OF THE PROPOSED ANTENNA

The equivalent circuit model for the proposed antenna is given below.

Table 1. Final optimized equivalent circuit model parameters.

Parameter	Value	Parameter	Value
L1	2.285 nH	**C1**	1.465 pF
L2	1.04 nH	**C2**	15.515 pF
L3	2.48 nH	**C3**	6.675 pF
L4	0.52 nH	**C4**	0.88 pF
L5	0.51 nH	**R1**	25 Ω
L6	0.496 nH	**R2**	70 Ω

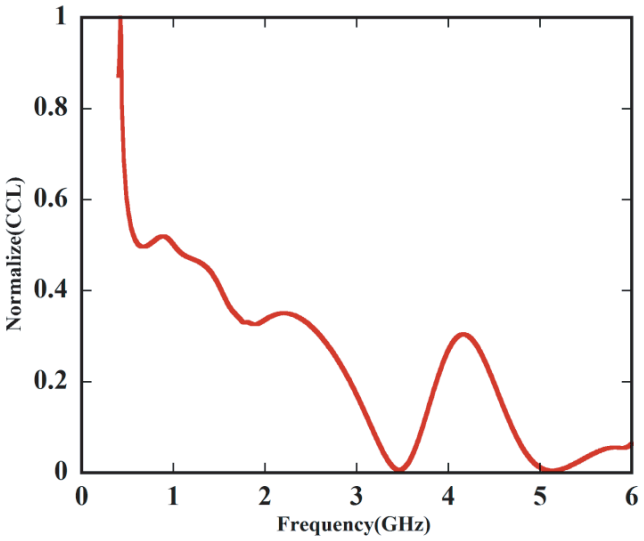

Figure 11. Simulated Channel capacity loss (CCL) of the proposed antenna.

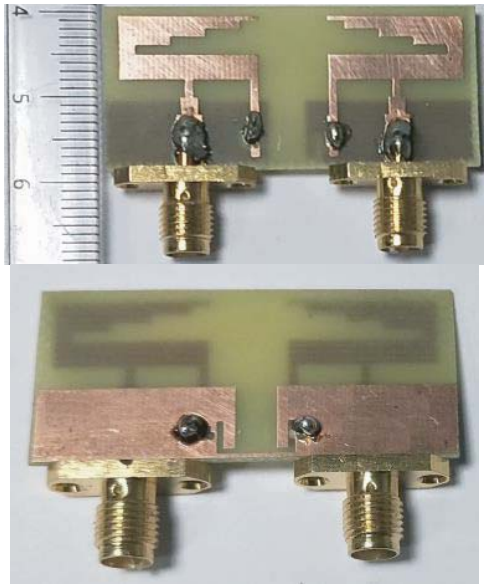

Figure 12. Top and bottom views of the fabricated prototype.

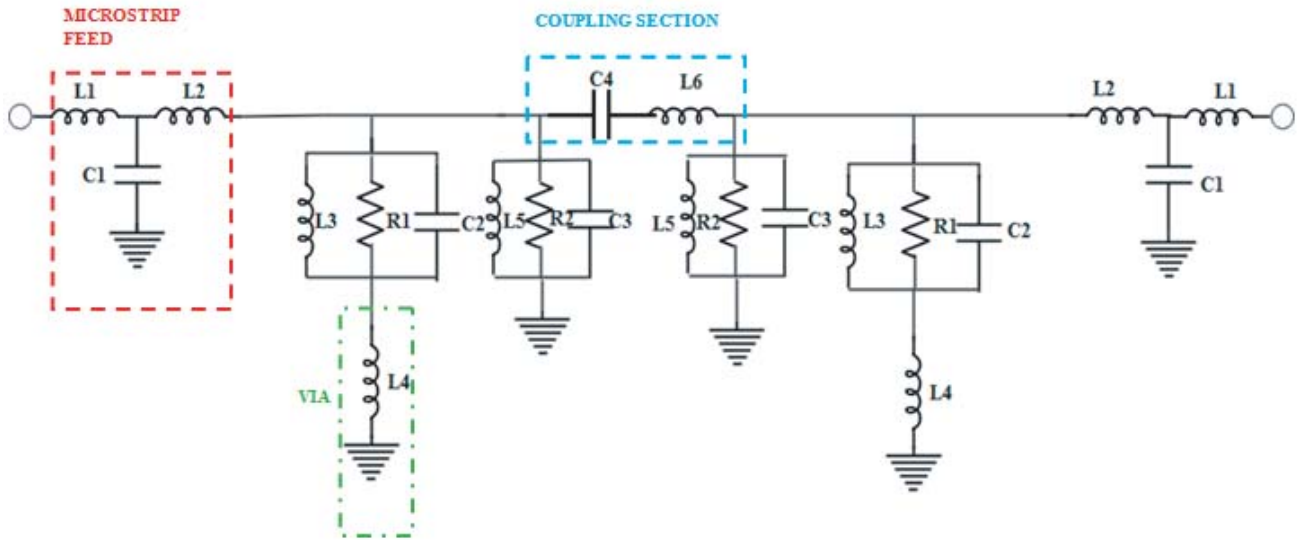

Figure 13. Equivalent circuit model.

The resonance behavior of the proposed dual-element MIMO antenna can be verified using the equivalent circuit analysis as shown in Figure 13. The values of L, C, and R are obtained by optimization operations in Keysight ADS software. The tuned values are tabulated in Table 1. The microstrip section is represented by L1 and C1. Power is coupled from the feeding section to the rest of the tank circuit through L2. Loading of a shorting pin with the patch introduces a parallel inductance L4. The two tank circuit is responsible for the dual bands. The effects of mutual coupling between ports 1 and 2 is represented by a series combination of L6 and C4. Figure 14 shows the simulated and measured results of the equivalent circuit model. It is observed that there is a good agreement between them.

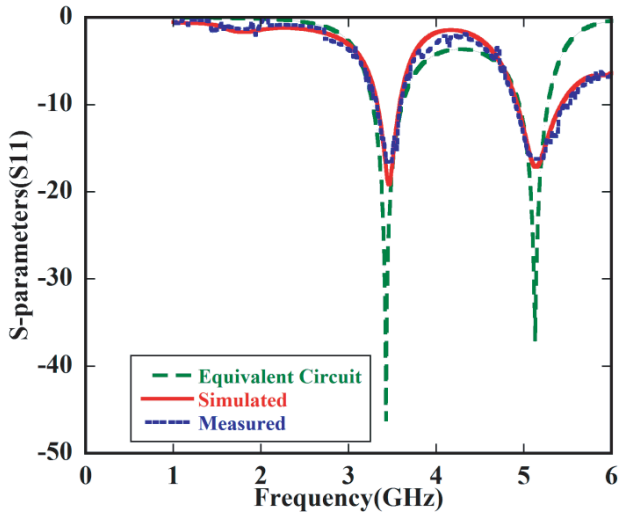

Figure 14. Equivalent circuit model, simulated and measured S_{11} of the proposed antenna.

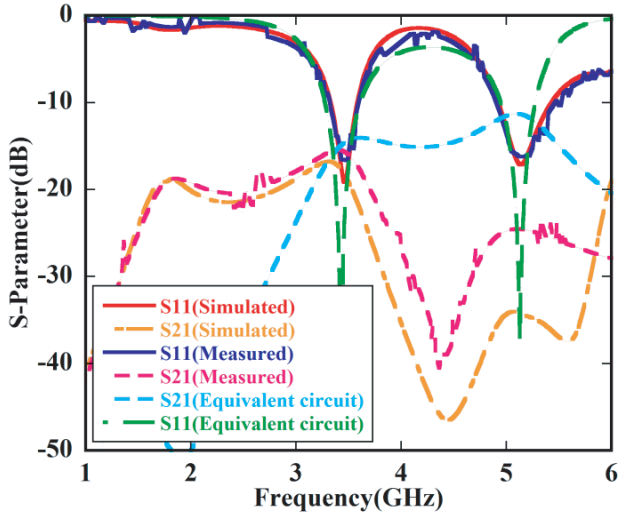

Figure 15. Simulated and measured $|S|$-parameters of the proposed MIMO antenna.

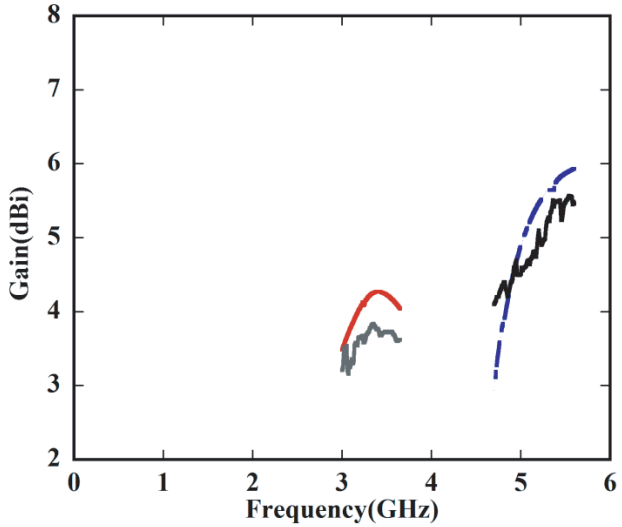

Figure 16. Simulated and measured peak gain.

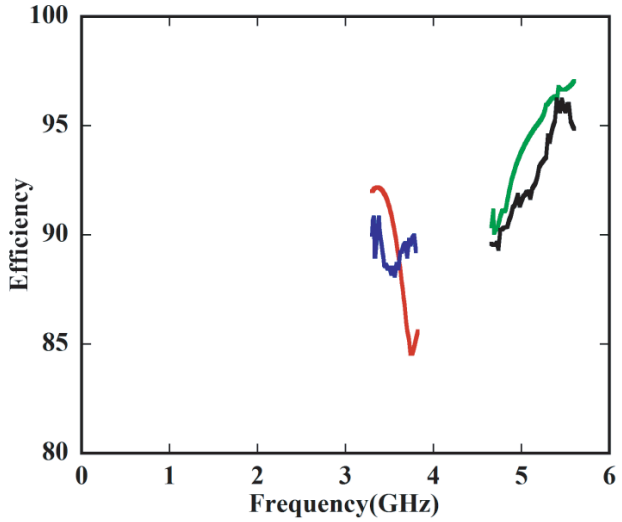

Figure 17. Simulated and measured radiation efficiency.

4. EXPERIMENTAL RESULTS AND DISCUSSION

A prototype of the proposed MIMO antenna is fabricated, and its $|S|$-parameters are measured. Both simulated and measured $|S|$-parameters are plotted in Figure 15, which show good agreement with slight discrepancies due to SMA connector loss and fabrication tolerances. The dual bands are (3.3 GHz–3.65 GHz) and (4.8 GHz–5.5 GHz), respectively.

The peak gains obtained at dual frequencies are 3.84 dBi and 5.93 dBi with radiation efficiencies of 92.2% and 97%, respectively as shown in Figures 16–17. Since the two antenna elements are same, only radiation pattern of ANT-I is measured, terminating ANT-II with matched load at 50 Ω. Figure 18 illustrates the simulated and measured radiation patterns, which include the co-polarization and cross-polarization, in the H-plane (X-Z plane) and E-plane (Y-Z plane). It can be noted that the radiation pattern in X-Z plane is nearly omnidirectional with cross polarization level within suitable

range. Table 2 compares the proposed structure with previously reported antennas having WLAN bands/5G band in terms of size, frequency of operation, isolation, ECC, gain, efficiency, and edge to edge separation. From the table, it is observed that the dimension of the proposed structure is compact as compared to other structures. In [4], a 1.6 mm thick FR-4 substrate is used making the overall size bigger than the proposed structure. Good isolation is achieved for the proposed structure, and ECC is also less than 0.002 thus can be practically acceptable for MIMO applications. Gains for both the bands are comparatively higher than the work referred in [3, 4, 11, 15]. The proposed antenna shows higher efficiency than [3, 5, 6, 11, 15]. One of the important parameters is the edge-edge separation; traditionally the minimum distance between the elements of a MIMO antenna should be half of the operating wavelength for desirable isolation and better performance. The inter element space for [3, 6, 7, 11] is very large, thus the structures are not compact. Though the inter element spacing for [4, 5] is less, the overall size is big.

Therefore, the proposed antenna design is the best trade-off while taking into account the aspect of size and the performance parameters which include isolation, ECC, gain, efficiency, and edge-to-edge separation, thus proving it to be the potential candidate in practical MIMO applications.

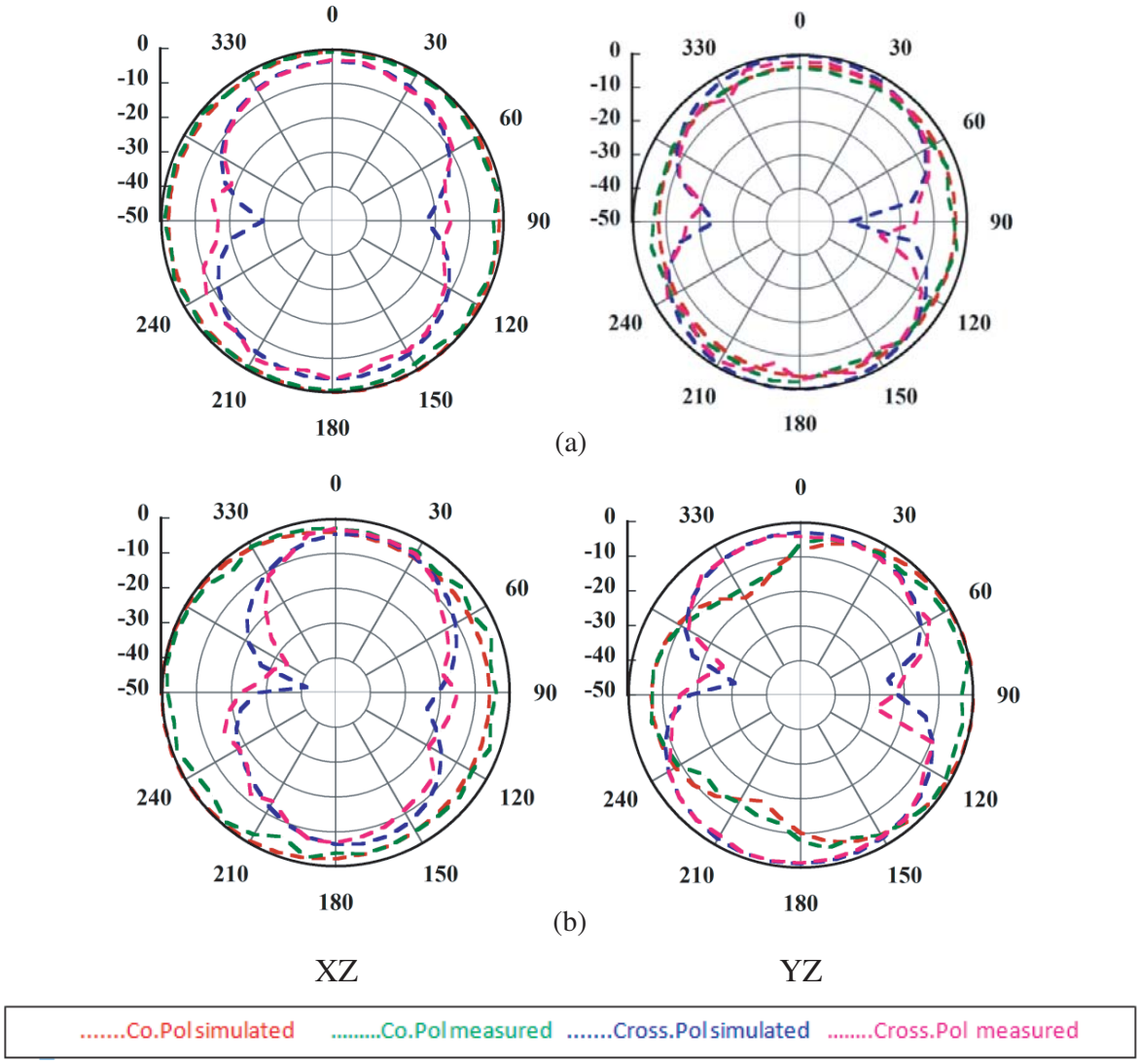

Figure 18. Simulated and measured normalized Radiation pattern in XZ and YZ plane. (a) 3.45 GHz. (b) 5.1 GHz.

Table 2. Comparison between the proposed antenna and similar reported two-element MIMO antenna.

Reference No.	Antenna size (mm × mm)	Frequency (GHz)	Isolation (dB)	ECC	Gain (dBi)	Efficiency (%)	Edge-to-Edge separation (mm)
3.	80 × 48	2.4/5	20, 21	< 0.01	4.7, 1.1	45.8, 40.6	14.4
4.	25 × 24	2.5/5.6	20, 22	< 0.004	0.28, 3.88		4
5.	100 × 5	2.4–2.5, 5.15–5.715.	30, 20	0.01, 0.2		92, 87	2
6.	77.5 × 52	2.4/5	Around 15 dB for both bands.	< 0.2		80	14.4
7.	60 × 6	2.4/5.2	25	< 0.08			15.3
11.	43 × 26	2.4, 3.5	32, 18	< 0.1	3.9, 4.2	75, (80–85)	10
15.	35 × 2	3.6	> 20	< 0.012	2.34	93.2	9
Proposed Antenna	**18 × 44**	**3.45, 5.1**	**18, 34**	**< 0.002**	**3.84, 5.93**	**92.2, 97**	**8**

5. CONCLUSION

The paper presents a new MIMO antenna for dual-band operation using IFA structure. The antenna uses a very simple decoupling structure based on a wide inverted T-shaped slot to achieve good isolation of ($|S_{21}| <= -18$ dB) and ($|S_{21}| <= -34$ dB) between the two ports at the dual frequencies, respectively. The antenna is very compact with an overall size of $(18 \times 44 \times 0.8)\,\text{mm}^3$. The operating bandwidth ($|S_{11}| <= -10$ dB) of the antenna is (3.3 GHz–3.65 GHz) and (4.8 GHz–5.5 GHz), respectively. The ECC, DG, and CCL are within acceptable limit. The gain is 3.84 dBi and 5.93 dBi for the dual frequencies with efficiencies 92.2% and 97%, respectively. The simulated, measured and equivalent circuit results also match well which confirms that the proposed antenna is a good candidate for 5G and WLAN applications.

REFERENCES

1. Steering Committee, "Making India 5G ready," Ministry of Communications, Delhi, India, 2018. URL: https://dot.gov.in/sites/default/files/5G%20Steering%20Committee%20report%20v%2026.pdf.
2. Telecom Regulatory Authority of India, "Enabling 5G in India," TRAI, Delhi, India, 2019. URL: https://trai.gov.in/sites/default/files/White_Paper_22022019_0.pdf.
3. Shen, D. L., L. Zhang, Y. C. Jiao, and Y. D. Yan, "Dual-element antenna with high isolation operating at the WLAN bands," *Microw. Opt. Technol. Lett.*, Vol. 61, 2323–2328, 2019.
4. Nandi, S. and A. Mohan, "A compact dual-band MIMO slot antenna for WLAN applications," *IEEE Antennas Wirel. Propag. Lett.*, Vol. 16, 2457–2460, 2017.
5. Addaci, R., K. Haneda, A. Diallo, P. L. Thuc, C. Luxey, R. Staraj, and P. Vainikainen, "Dual-band WLAN multiantenna system and diversity/MIMO performance evaluation," *IEEE Trans. Antennas Propag.*, Vol. 62, 1409–1415, 2014.
6. Deng, J. Y., J. Y. Li, L. Zhao, and L. X. Guo, "A dual-band inverted-F MIMO antenna with enhanced isolation for WLAN applications," *IEEE Antennas Wirel. Propag. Lett.*, Vol. 16, 2270–2273, 2017.
7. Deng, J. Y., Z. J. Wang, J. Y. Li, and L. X. Guo, "A dual-band MIMO antenna decoupled by a meandering line resonator for WLAN applications," *Microw. Opt. Technol. Lett.*, Vol. 60, 759–765, 2018.

8. Cui, S., Y. Liu, W. Jiang, S. X. Gong, Y. Guan, and S. T. Yu, "A novel compact dualband MIMO antenna with high port isolation," *Journal of Electromagnetic Waves and Applications*, Vol. 25, Nos. 11–12, 1645–1655, 2011.
9. Qin, H. and Y. F. Liu, "Compact dual-band MIMO antenna with high port isolation for WLAN applications," *Progress In Electromagnetics Research C*, Vol. 49, 97–104, 2014.
10. Sharawi, M. S., M. A. Jan, and D. N. Aloi, "Four-shaped 2×2 multi-standard compact multiple-input-multiple-output antenna system for long-term evolution mobile handsets," *IET Microw. Antennas Propag.*, Vol. 6, No. 6, 685–696, 2012.
11. Panda, A. K., S. Sahu, and R. K. Mishra, "A compact dual-band 2×1 metamaterial inspired mimo antenna system with high port isolation for LTE and WiMax applications," *Int. J. RF Microw. Comput. Aided Eng.*, Vol. 00, e21122, 2017.
12. Liu, Y., Y. Wang, and Z. Du, "A broadband dual-antenna system operating at the WLAN/WiMax bands for laptop computers," *IEEE Antennas Wirel. Propag. Lett.*, Vol. 14, 1060–1063, 2015.
13. Guo, L., Y. Wang, Z. Du, Y. G. Gao, and D. Shi, "A compact uniplanar printed dual-antenna operating at the 2.4/5.2/5.8 GHz WLAN bands for laptop computers," *IEEE Antennas Wirel. Propag. Lett.*, Vol. 13, 229–232, 2014.
14. Liu, Y., L. Yang, Y. Liu, J. Ren, J. Wang, and X. Li, "Dual-band planar MIMO antenna for WLAN application," *Microw. Opt. Technol. Lett.*, Vol. 57, 2257–2262, 2015.
15. Saurabh, A. K. and M. K. Meshram, "Compact sub-6 GHz 5G-multipleinput-multiple-output antenna system with enhanced isolation," *Int. J. RF Microw. Comput. Aided Eng.*, e22246, 2020.
16. Roy, S., A. K. Biswas, S. Ghosh, U. Chakraborty, and A. Sarkhel, "Isolation improvement of dual-/quad-element textile MIMO antenna for 5G application," *Journal of Electromagnetic Waves and Applications*, Vol. 35, No. 10, 1337–1353, 2021.
17. Yuan, X. T., Z. Chen, T. Gu, and T. Yuan, "A wideband PIFA-pair-based MIMO antenna for 5G smartphones," *IEEE Antennas Wirel. Propag. Lett.*, Vol. 20, 371–375, 2021.
18. Bartwal, P., A. K. Gautam, A. K. Singh, B. K. Kanaujia, and K. Rambabu, "Design of compact multi-band meander-line antenna for global positioning system/wireless local area network/worldwide interoperability for microwave access band applications in laptops/tablets," *IET Microw. Antennas Propag.*, Vol. 10, 1618–1624, 2016.
19. Chatterjee, A., M. Midya, L. Prasad Mishra, and M. Mitra, "Branch line strip loaded compact printed Inverted-F Antenna (IFA) for penta-band applications," *International Journal of Electronics and Communications*, 2020, doi: https://doi.org/10.1016/j.aeue.2020.153340.
20. Kuo, Y. L. and K. L. Wong, "Coplanar waveguide-fed folded inverted-F antenna for UMTS applications," *Microw. Opt. Technol. Lett.*, Vol. 32, No. 5, 364–366, 2002.
21. Thakur, E., N. Jaglan, and S. D. Gupta, "Design of compact UWB MIMO antenna with enhanced bandwidth," *Progress In Electromagnetics Research C*, Vol. 97, 83–94, 2019.
22. Gurjar, R., D. K. Upadhyay, B. K. Kanaujia, and K. Sharma, "A novel compact self-similar fractal UWB MIMO antenna," *Int. J. RF Microw. Comput. Aided Eng.*, Vol. 29, No. 3, e21632, 2019.